Geophysical Research Letters

RESEARCH LETTER
10.1029/2022GL101500

Interdecadal Pacific Oscillation in Northern Greenland Dust Concentration Variability During the Last 400 Years

N. Rimbu[1], M. Ionita[1,2,3], and G. Lohmann[1,4]

[1]Alfred Wegener Institute Helmholtz Center for Polar and Marine Research, Bremerhaven, Germany, [2]Emil Racovita Institute of Speleology, Romanian Academy, Cluj-Napoca, Romania, [3]Faculty of Forestry, "Stefan cel Mare" University of Suceava, Suceava, Romania, [4]Physics Department & MARUM, University of Bremen, Bremen, Germany

Abstract Statistical analysis of reanalysis and observed data reveals that high dust surface mass concentration in northern Greenland is associated with a Pacific Decadal Oscillation like pattern in its negative phase in the North Pacific as well as with La Niña conditions in the tropical Pacific region. The sea surface temperature anomalies in the Pacific realm resemble the Interdecadal Pacific Oscillation (IPO). The associated atmospheric circulation pattern, in the form of a wave-train from the North Pacific to the Eurasian continent, favors enhanced dust uptake and transport toward the northern Greenland. Similar patterns are associated with a low-resolution stacked record of five Ca^{2+} ice cores, that is, ngt03C93.2 (B16), ngt14C93.2 (B18), ngt27C94.2 (B21), GISP2−B, and NEEM-2011-S1, from northern Greenland, a proxy for regional dust concentration, during the last 400 years. We argue that northern Greenland ice core dust records could be used as proxies for the IPO and related teleconnections.

Plain Language Summary Observational and modeling studies show that, during the observational period, interannual to multidecadal dust concentration variability is related to the dominant modes of climate variability at these time scales. Here we show that Interdecadal Pacific Oscillation (IPO) signal is robustly recorded in low-resolution dust ice core records from the northern Greenland during the last 400 years. We argue that northern Greenland ice core dust records could be used to put the IPO activity and related teleconnections during the observational period into a long-term perspective.

Key Points:

- Northern Greenland dust concentration variability shows global teleconnections during the instrumental period
- The most stable pattern associated with northern Greenland ice core dust variability is the Interdecadal Pacific Oscillation (IPO)
- Northern Greenland ice core dust records could be used as a complementary source of information about IPO during the past

Supporting Information:

Supporting Information may be found in the online version of this article.

Correspondence to:

N. Rimbu,
Norel.Rimbu@awi.de

Citation:

Rimbu, N., Ionita, M., & Lohmann, G. (2022). Interdecadal Pacific Oscillation in northern Greenland dust concentration variability during the last 400 years. *Geophysical Research Letters*, *49*, e2022GL101500. https://doi.org/10.1029/2022GL101500

Received 3 OCT 2022
Accepted 9 DEC 2022

Author Contributions:

Conceptualization: N. Rimbu, G. Lohmann
Formal analysis: N. Rimbu
Funding acquisition: M. Ionita
Investigation: M. Ionita
Methodology: N. Rimbu, G. Lohmann
Supervision: G. Lohmann
Visualization: M. Ionita

1. Introduction

The concentration of mineral dust aerosol, a suspension of tiny soil particles in the atmosphere, is highly sensitive to climate and environmental changes. Recent studies report significant interannual to decadal variability in observed and proxy dust concentration records from Greenland (Bullard & Mockford, 2018; Kjaer et al., 2022; Nagatsuka et al., 2021), Europe (Clifford et al., 2019) or Middle-East (Notaro et al., 2015; Yu et al., 2015) during the observational period. Strong variability in the dust concentration at longer time scales, that is, centennial to millennial, are detected in ice core records from the Arctic region (Fuhrer et al., 1999; Legrand & Mayewski, 1997; Rasmussen et al., 2014). Overall, the variability and change in the dust concentration have been related both with natural and anthropogenic forcing (e.g., IPCC, 2007).

Analysis of observational data and model experiments reveal that large-scale climatic patterns modulate the dust up-take and transport pathways. The African dust transport, for example, is modulated by the position and strength of the Azores High, which is related to the North Atlantic Oscillation (e.g., Chiapello et al., 2005). The Arctic Oscillation was related to East Asia dust activity and associated weather disturbances (Gong et al., 2006). The dust export rate toward the subtropical North Atlantic is significantly correlated with the North African dipole index (Rodriguez et al., 2015), a quantity which reflects the meridional pressure gradient across North Africa. The dust activity over the US was related to the phase of the relevant modes of climate variability like El Niño-Southern Oscillation (ENSO) or Pacific Decadal Oscillation (PDO) (Hand et al., 2016). Furthermore, the PDO was related to dust activity in the Middle-East during the spring (Pu & Ginoux, 2016). Recently, reanalysis aerosol products have been used to investigate the impact of the climate modes, like ENSO and PDO, in dust concentration variability on regional and global scale (e.g., Shi et al., 2022). In line with these studies, here we investigate the large-scale climate anomalies associated with northern Greenland dust concentration variability using various observational, reanalysis and ice core dust records. The focus is in the teleconnections of northern Greenland dust concentration variability with Pacific decadal to multidecadal variability, in particular on

Interdecadal Pacific Oscillation (IPO). Understanding the northern Greenland surface dust concentration variability during the observational period is useful for a proper interpretation of northern Greenland ice core dust proxy record variability and its teleconnections during the past.

Ice core records from northern Greenland are a rich source of information about dust concentration variability in the region from interannual to multi-millennial time scales (e.g., Fuhrer et al., 1999; Steffensen, 1997). Previous studies (Bory et al., 2002; Fischer et al., 2007; Rasmussen et al., 2014) indicate that the Ca^{2+} in polar ice cores is a good proxy for the terrestrial dust source. We therefore treat the Ca^{2+} from northern Greenland ice core records analyzed here as a proxy for the amount of terrestrial dust, while realizing that the sea salt may also be present (Legrand & Mayewski, 1997). We combine the ice core records with paleo-reanalysis data to identify the global-scale climate anomalies associated with the ice core variability.

The main goal of our study is to put the relationships between the northern Greenland dust concentration variability and large-scale modes of interannual to decadal variability during the observational period into a long-term perspective using long-term observational, proxy as well as paleo-reanalysis data. We will show that interannual to multidecadal northern Greenland dust variability, as recorded in five ice cores from the region, is related to a global-scale sea surface temperature anomaly pattern having a strong imprint of the IPO in the Pacific Ocean. We argue that dust records from northern Greenland ice cores could be used not only to improve but also to extend back in time the existing IPO reconstructions, as described in recent studies (e.g., Porter et al., 2021).

2. Data and Methods

Modern-Era Retrospective Analysis for Research and Applications version 2 (MERRA-2) is a long-term atmospheric reanalysis since 1980 (e.g., Gelaro et al., 2017). The MERRA-2 data is often used for investigation the aerosol variability and related large-scale teleconnections (e.g., Shi et al., 2022). Here we use monthly mean dust surface mass concentration (DUSMASS) field retrieved from MERRA-2 web page (https://gmao.gsfc.nasa.gov/reanalysis/MERRA-2/), contained in the tavgM_2d_aer_Nx (M2TMNXAER; https://doi.org/10.5067/FH9A0MLJPC7N) data set. The monthly mean fields of the 500 hPa geopotential height (Z500) and wind fields for the 1980–2018 period were retrieved also from the MERRA-2 database. Our study is focused on the interannual to decadal variability of the northern Greenland spring ((March-April-May (MAM)) dust surface mass concentration and its global teleconnections from 1980 to 2018. The centennial in situ observation-based estimates (COBE) sea surface temperature (SST) data set (e.g., Ishii et al., 2005) provided by NOAA/OAR/ESRL PSL, Boulder, Colorado, USA (https://psl.noaa.gov/), is used to derive global SST anomaly patterns associated with northern Greenland surface mass concentration variability during this period, that is, from 1980 to 2018.

The IPO index used in this study is defined as the difference between normalized SST anomalies over a central equatorial Pacific region, that is, (170°E−90°W; 10°S–10°N) and the average of normalized SST anomalies in the northwest (25°N–45°N; 140°E−145°W) and southwest (150°E−160°W; 50°S–15°S) Pacific. This index, defined by Henley et al. (2015), was calculated using the COBE SST data set (e.g., Ishii et al., 2005). We also made use of the long-term (back to 1891) monthly Niño34 and PDO indices, which are calculated also using the COBE SST data set (Ishii et al., 2005). The Niño34 index is defined as the average of SST anomalies within the region 170°W–120°W and 5°S–5°N, while the PDO index is defined as the first principal component (PC1) of the SST anomalies over the North Pacific Ocean. The Z500 and wind fields, retrieved from 20CRv2c reanalysis (Compo et al., 2011), are used to derive the atmospheric circulation patterns associated with ice core record back to 1891.

Five Ca^{2+} records from northern Greenland (Figure S1a in Supporting Information S1) are used in this study. The ngt03C93.2 (B16) (Fischer, 2000a), ngt14C93.2(B18) (Fischer, 2003), ngt27C94.2 (B21) (Fischer, 2000b) and GISP2−B (Mayewski, 1999) were downloaded from the environmental database PANGAEA (www.pangaea.de). The NEEM-2011-S1 record (McConell, 2013) was downloaded from the Arctic Data Center (https://arctic-data.io/). These records will be referred hereafter as B16, B18, B21, GISP2 and NEEM-S1. The B21 (80.00°N; 41.14°W, 2185 masl) extends from 1397 AD to 1991 AD, B18 (76.61°N; 36.40°W, 2508 masl) from 1442 AD to 1991 AD and B16 (73.94°N; 37.63°W, 3040 masl) from 1481 AD to 1991 AD. All these three records have a 3-year temporal resolution. The GISP2b record (72.58°N; 38.45°W, 3203 masl) covers the period 1271 AD to 1987 AD with a bi-yearly resolution. The NEEM-S1 Ca^{2+} record (77.45°N, 51.06°W, 2450 masl) covers the period 77 AD to 1997 AD with higher than seasonal resolution. We choose these records not only because of

their availability, but also because they are well established records for dust concentration in northern Greenland ice cores. Our analysis is limited to the period covered by all these records and paleo-reanalysis data used here (Valler et al., 2021), which is 1603 AD to 1992 AD. These ice core records are weakly positively correlated each other ($r \sim 0.1$), over this period, suggesting a possible common climate forcing on northern Greenland dust concentration variability during the last 400 years. The 3-year resolution time series as well as the stacked (average) record over this period shows pronounced decadal to multidecadal variations (Figure S1b in Supporting Information S1).

Paleo-proxy data assimilation systems use climate models and multi-proxy networks to produce gridded data sets of climate variables (hereafter paleo-reanalysis). Here we use the 2 m temperature (T) and Z500 fields from the recently published EKF400v2 paleo-reanalysis data set (Valler et al., 2021). The EKF4000v2 covers the period 1602 AD to 2003 AD with monthly resolution. From monthly mean data, we calculate the average of spring data as the average of March, April, and May (MAM) for each year. Furthermore, the averages of three consecutive springs are used in a composite analysis. The linear trend was removed from data prior to any statistical analysis. The reconstructed IPO index over the last centuries (Porter et al., 2021), is used to test the robustness of the IPO signal in our ice core records during the last four centuries.

The climate anomaly patterns are derived through composite and analysis (e.g., von Storch & Zwiers, 1999). Climate anomaly maps corresponding to the time when a certain index is higher (lower) than +0.5 (−0.5) standard deviation are averaged. The difference between high and low averaged maps are referred to as composite map and the difference values as anomalies. The significance of the anomalies is based on a simple *t*-test (e.g., von Storch & Zwiers, 1999).

3. Results

3.1. Northern Greenland Dust Teleconnections in MERRA-2 Reanalysis

First, we investigate the large-scale teleconnections of the northern Greenland dust variability during 1980–2018, using present-day dust concentration data from the MERRA-2 reanalysis data set (Gelaro et al., 2017) as well as observed global SST and climate indices. The analysis focuses on the spring season (MAM), when the dust deposition is peaking in Greenland ice cores (Bory et al., 2002; Hamilton & Langway, 1967) and the Northern Hemisphere dust activity is the highest (e.g., Prospero et al., 2002). Note, that 3-year resolution data, that is, the average over three consecutive springs, are used in the statistical analysis, to have the same resolution as ice-core data.

To analyze the relationship between the dust variability over Greenland and the large-scale atmospheric and oceanic circulation, we define an index as the average of spring dust surface mass concentration, that is, the DUSMASS variable from MERRA-2 data set, for all grid-points within the region (55°W–20°W; 70°N–85°N) (Figure 1a; rectangle box). All the five ice cores considered here are located within this region (Figure S1a in Supporting Information S1). The SST composite map associated with this index shows large-scale structures reminiscent of pre-defined teleconnection patterns. Highly significant positive SST anomalies are recorded in the North Atlantic region, south of Greenland. The global SST anomaly pattern contains also elements of the PDO in its negative phase, in the North Pacific, as well as elements of the negative phase of ENSO, that is, La Niña phase, in the tropical Pacific (Figure 1a). This suggests that both ENSO and PDO control part of northern Greenland interannual to decadal dust concentration variability. A simple visual inspection of Niño34 and PDO indices during this period (Figure S2 in Supporting Information S1) reveals that high (low) surface mass dust concentration is recorded frequently during La Niña (El Niño) years, that is, 1985, 1989, 2001, and 2008 (1983, 1992, 2015, and 2016). Consistent with this, the spring mean time series of dust concentration and the Niño34 and the PDO indices, are significantly negatively correlated ($r = -0.43$ and -0.52 respectively, $p < 0.01$) over the period 1980–2018 (Figure S2 in Supporting Information S1). Over the Pacific Ocean, the SST anomaly pattern associated with northern Greenland dust concentration variability has a basin wide horseshoe shape reminiscent to the negative phase of the IPO (Figure 1a). This is consistent with significant negative correlation ($r = -0.62$) between northern Greenland dust concentration and IPO indices at decadal time scales (Figure S3 in Supporting Information S1).

Consistent with the SST composite map (Figure 1a), the 500 hPa atmospheric circulation anomaly pattern associated with the northern Greenland surface dust mass concentration index shows also large-scale features (Figure 1b). Negative Z500 anomalies prevail in the tropical region, consistent with La Niña conditions in the

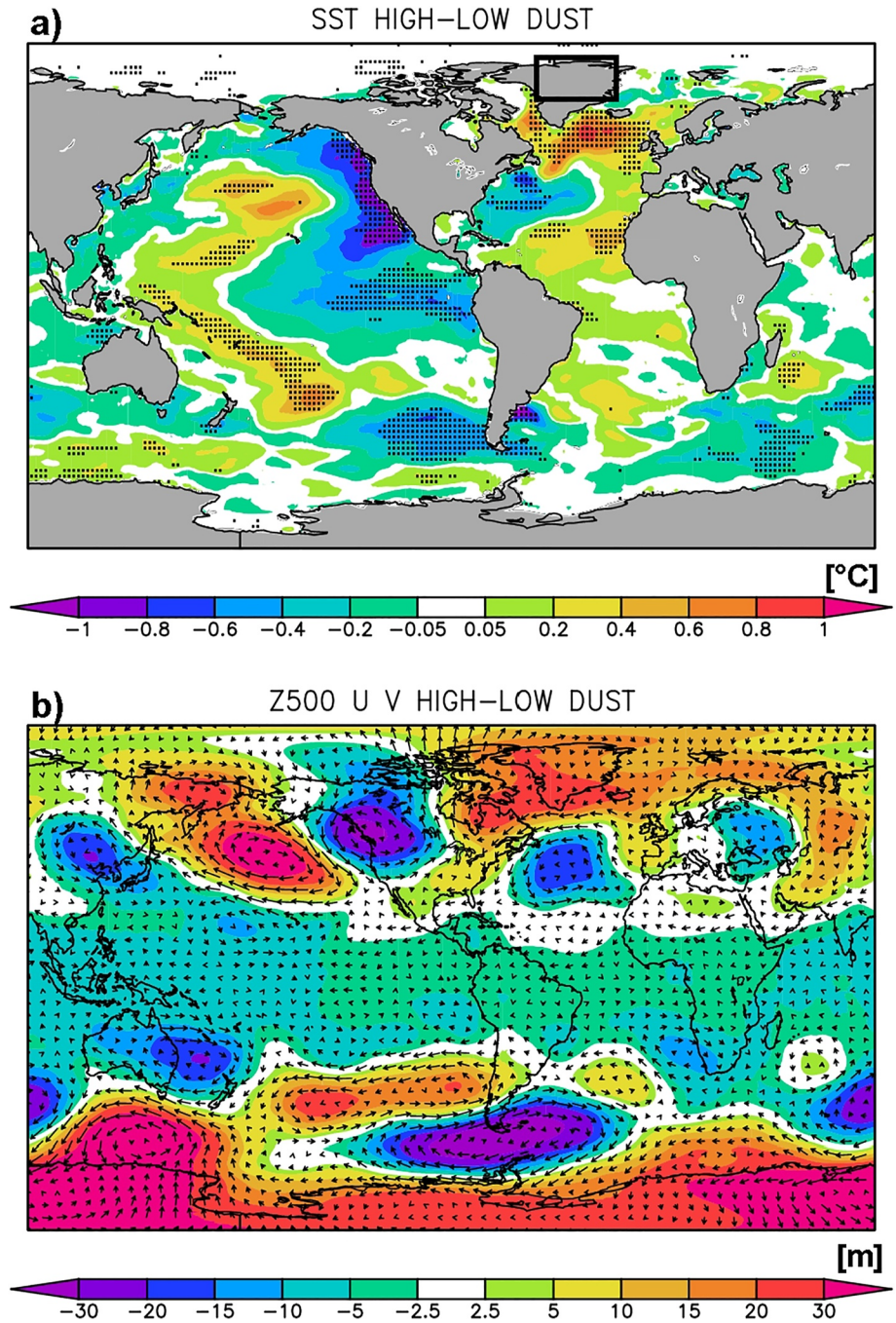

Figure 1. (a) The composite map (High—Low) of the SST associated with high and low values of the northern Greenland dust index (see text for definition). The rectangle box represents the dust index region and (b) The corresponding Z500 (color) and wind (vector) anomalies. Regions where the SST anomalies are significant at the 90% level (based on a two-tail *t*-test) are dotted. 3-year resolution spring data are used in the analysis. Units: SST (°C) and Z500 (m).

tropical Pacific. A wave-train pattern, with positive anomalies over the North Pacific and Florida region and negative over North America, dominates the Pacific North American (PNA) sector. It contains elements of classical PNA pattern (e.g., Wallace & Gutzler, 1981) in its negative phase, which is enhanced during La Niña years. The structure of Z500 anomalies over the Eurasian continent (Figure 1b) shows negative anomalies over the Eastern Europe—western Russia and South East Asia, suggesting enhanced cyclonic activity in these regions during high dust concentration periods in northern Greenland. For example, spring dust storms in the Gobi desert

are generated by cold air outbreaks associated with strong low-pressure systems during the passage of cold fronts (e.g., Huang et al., 2015). The negative Z500 anomalies over East Asia (Figure 1b) suggest an enhanced East Asian Trough (EAT) during high dust surface mass concentration in northern Greenland. It was shown that an enhanced EAT favors the transport of dust by the cyclones toward the Arctic region (Huang et al., 2015). Furthermore, the intensity of EAT, in a specific atmospheric circulation context, is strongly modulated by ENSO (Yu & Sun, 2020). To sum up, the structure of the Z500 anomalies in the Eurasian region (Figure 1b) suggests that enhanced dust transport to northern Greenland from the main Northern Hemisphere dust source regions, that is, northern Africa, Middle East, and Central and East Asia regions, occurs both via North Atlantic or via North Pacific. Both paths were identified as possible routes of Saharan or Central Asia dust in the Arctic region at the synoptic scale (Francis et al., 2019; Huang et al., 2015).

3.2. Teleconnections in Proxy Data Records

Statistical analysis of observational and reanalysis data, presented above, reveals that northern Greenland dust surface mass concentration is relatively high (low) during the negative (positive) IPO phase. In the following we want to see if this relationship could be identified also over longer timescales by employing low-resolution ice core dust records from northern Greenland and global paleo-reanalysis data.

The ice core records considered in our study have higher than seasonal (NEEM-S1), ∼bi-yearly (GISP2) and three-yearly (B16, B18, and B21) resolutions. We calculate the average of NEEM-S1 and GISP2 values in 3-year bins centered on the B16 time points to have 3-year resolution records. A simple visual inspection of these records (Figure S1b in Supporting Information S1) reveals some common signals in all records, like a negative trend and enhanced multidecadal variability after the 1850s. Also, periods when low (high) values prevail in all ice core records, like 1620's and 1850's (1650's and 1940's), can be identified. These five records were averaged (stacked) to improve signal-to-noise ratio. The resulted time series (Figure S1b (thick line) in Supporting Information S1) shows pronounced decadal to multidecadal variations during the last four hundred years. Note a decreasing trend in the averaged record since the 1850s. Interestingly, a positive trend since 1850s was identified in a reconstruction of the IPO index (Porter et al., 2021).

The composite map of the SST (Figure 2a), based on the stacked record for the period 1891 to 1992, shows that high dust concentration in Greenland ice cores is associated with an IPO like pattern in its negative phase in the Pacific, similar to observations (Figure 1a). Consistent with this, the IPO index is significantly negatively correlated ($r = -0.56$; $p < 0.01$) with the ice core record (Figure S4 in Supporting Information S1). The composite map of Z500 (Figure 2b) shows a negative phase PNA-like pattern in the north Pacific, like in observations (Figure 1b). Similar to observations (Figure 1b) the Arctic region of the Eurasian continent is dominated by positive anomalies. Two negative centers of Z500 over the central north Atlantic and western Europe are also recorded (Figure 2b). The negative anomalies over East Asia suggests an enhanced EAT (Figure 2b). The Z500 anomaly pattern (Figure 2b), similar to observations, suggests also enhanced cyclonic activity over the North Africa and Middle-East, that is, strong dust uptake from these regions, as well as enhanced dust transport toward Greenland, both via North Atlantic and North Pacific routes.

Similar Pacific temperature (Figure 3a) and Z500 (Figure 3b) patterns emerge from a composite analysis of the ice core and paleo-reanalysis data (Valler et al., 2021) for the period 1603 AD to 1992 AD. The IPO index, calculated based on paleo-reanalysis temperature data (Valler et al., 2021) is significantly negatively correlated ($r = -0.31$) with dust ice core record (Figure 4), consistent with the composite map of the temperature for this period (Figure 3a). Note, relatively strong multidecadal variations after 1750's in both time series with clear out of phase variations during persistent IPO events. Before 1750's the multidecadal variability is relatively absent (Figure 4). A similar behavior is reported for a recent IPO reconstruction (Porter et al., 2021). The correlation map of Ca^{2+} time series and global 2 m temperature field over the entire 1603–1992 period shows a clear IPO pattern in the Pacific realm (Figure S5a in Supporting Information S1). Similar patterns are obtained for the period 1603–1782 and 1813–1992 (Figures S5b and S5c in Supporting Information S1), when the Ca^{2+} stacked record was dominated by interannual to decadal and respectively multidecadal variability (Figure 4). This shows that the IPO signal in our ice core records is robust during the analyzed period.

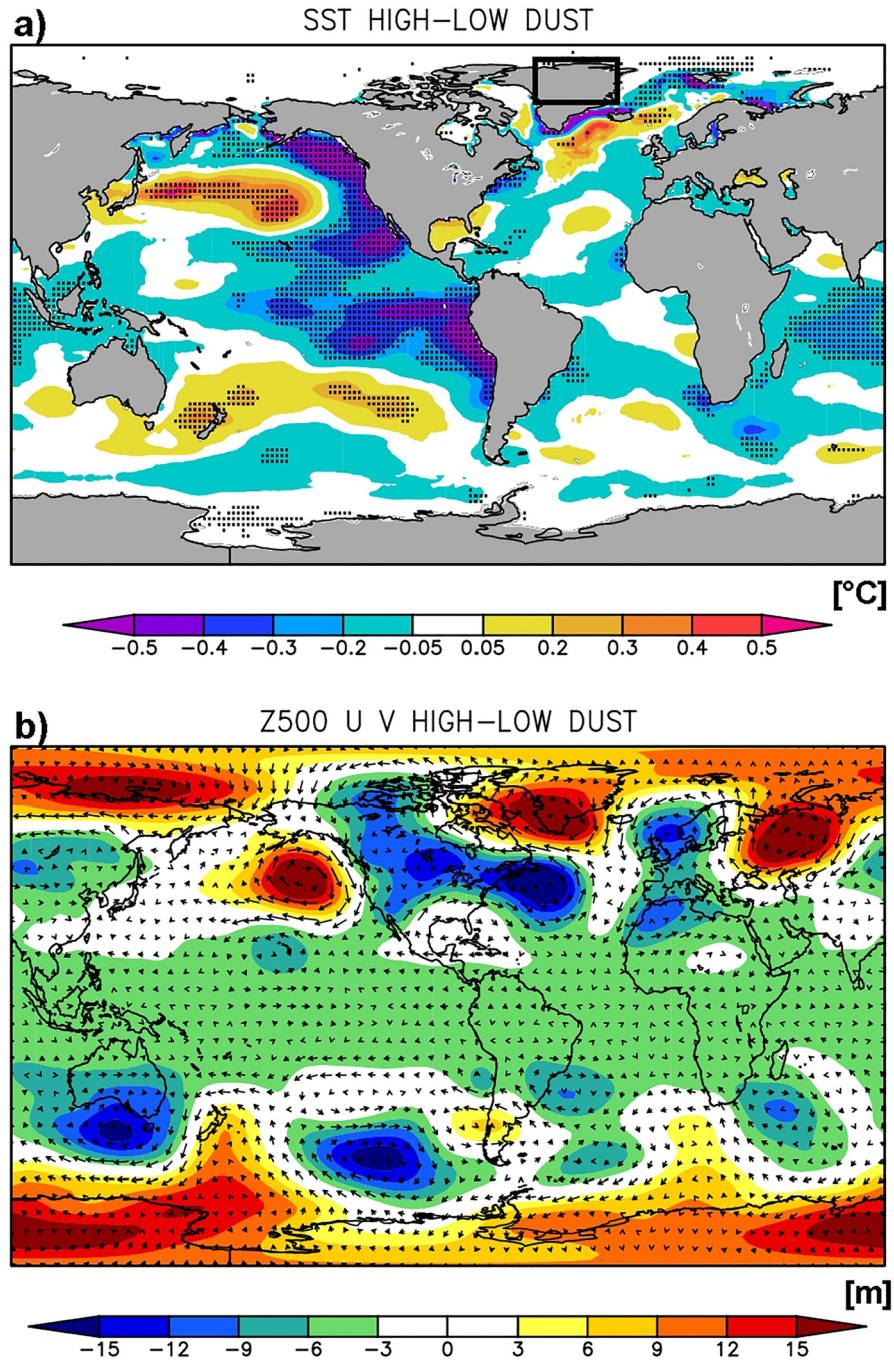

Figure 2. (a) The composite map (High—Low) of the SST associated with high and low values of the northern Greenland Ca^{2+} ice core record (see text for details) during 1891–1992 and (b) The corresponding Z500 (color) and wind (vector) anomaly patterns. Regions where the SST anomalies are significant at the 90% level (based on a two-tail *t*-test) are dotted. 3-year resolution spring data are used in the analysis. Units: SST (°C) and Z500 (m).

4. Discussions and Conclusions

In this study, we have investigated the global atmospheric teleconnections associated with the variability of northern Greenland dust concentration during the instrumental and pre-instrumental periods. We have shown that during 1980–2018 period, high dust surface mass concentration in northern Greenland is associated with significant positive SST anomalies south of Greenland, La Niña conditions in the tropical region as well as a negative PDO SST like pattern in the North Pacific. The corresponding atmospheric circulations show a wave-train pattern

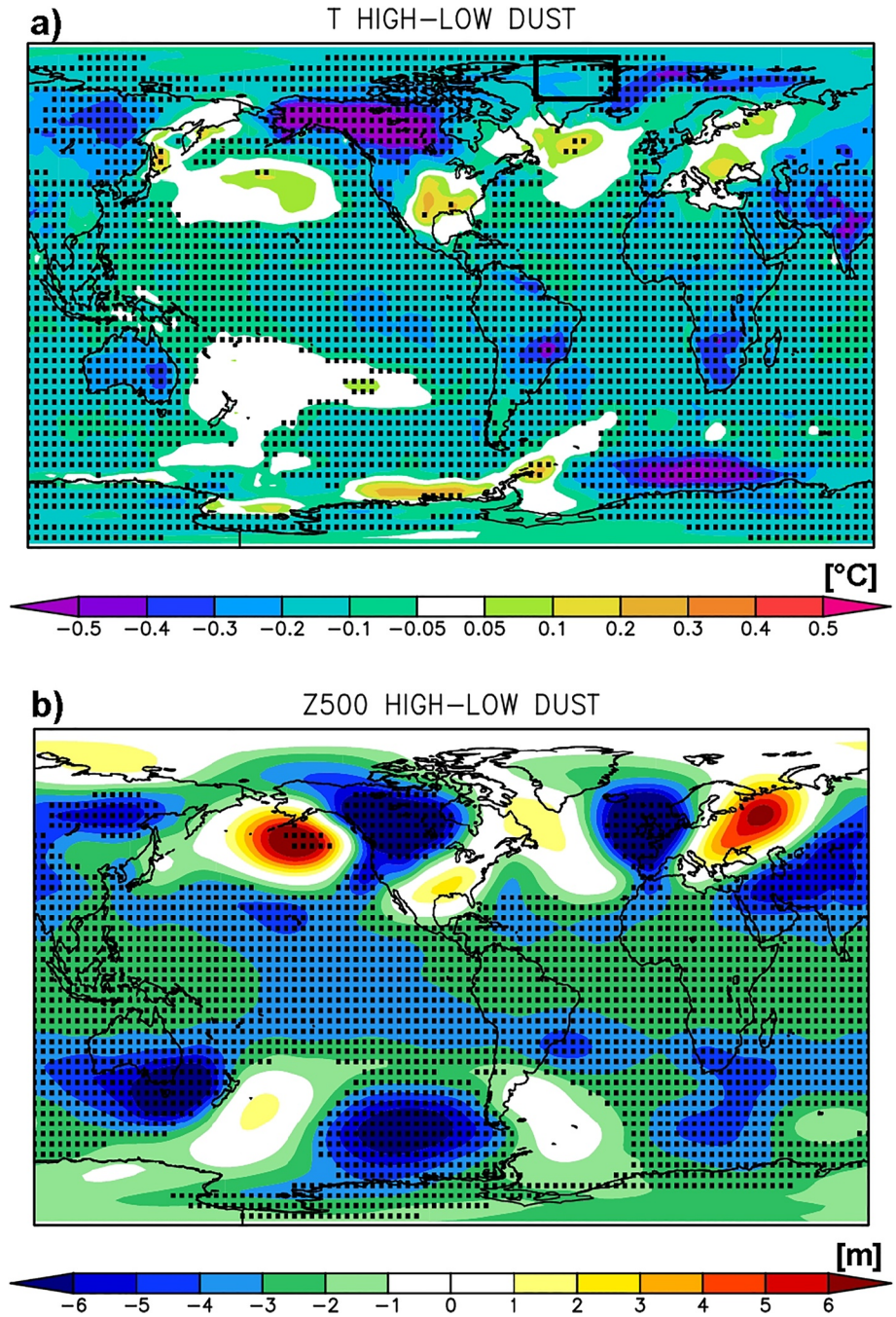

Figure 3. (a) The composite map (High—Low) of the air temperature associated with high and low values of the northern Greenland Ca^{2+} ice core record (see text for details) during 1602–1992. (b) The corresponding Z500 anomaly pattern. Regions where the anomalies are significant at the 90% level (based on a two-tail *t*-test) are dotted. 3-year resolution spring data are used in the analysis. Units: T (°C) and Z500 (m).

in the PNA region and more regional and variable features in the Eurasian region. These anomalous atmospheric circulations are consistent with enhanced dust uptake and long-range transport of dust from the Northern Hemisphere main sources to the Arctic during the negative phase of the IPO. The Pacific SST pattern remains qualitatively the same from interannual to multidecadal variability both in observed and paleo-reanalysis data.

Model studies (Kok et al., 2021) suggest a large variety of dust sources for the Greenland dust deposition flux. Important contributors to northern Greenland dust are North Africa, East Asia and North America. Dust

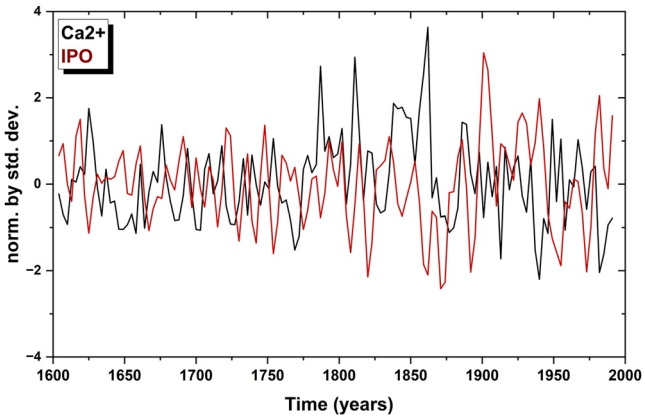

Figure 4. Time series of northern Greenland stacked ice core dust record (black) and the Interdecadal Pacific Oscillation (IPO) index (red) during 1602–1992. The IPO index has a 3-year resolution (average over three consecutive springs).

from higher-latitudes, for example, northwestern Greenland (Bullard & Mockford, 2018), could also contribute to northern Greenland dust concentration. The atmospheric circulation patterns associated with both observed and ice core-based dust records presented here are consistent with these large variety of dust sources for northern Greenland. However, the most robust teleconnection of northern Greenland dust variability is with the Pacific realm. The negative phase of the IPO associated with a PNA-like pattern in the American-North Pacific region are clearly identified both in observed and proxy based composites. More complex and variable patterns are obtained for the Eurasian continent. This could be due to non-stationary ENSO impact on Eurasian dust activity (Shi et al., 2022). Non-stationary teleconnections between other modes of climate variability, like PDO, could also explain the atmospheric circulation patterns over the Eurasian region associated with northern Greenland dust variability. Furthermore, the intensity of EAT, an important pattern for dust transport from East Asia to the Arctic region (Huang et al., 2015), which is enhanced during high dust concentration in northern Greenland, is related to ENSO activity in the tropical Pacific (Yu & Sun, 2020).

The strength of ENSO-EAT relationship depends on the phase of the North Pacific Oscillation and Asian Polar Vortex (Yu & Sun, 2020). The atmospheric circulation patterns associated with northern Greenland dust concentration variability (Figure 1b) and dust ice core records (Figure 2b) are consistent with ENSO-EAT teleconnections during the observational period. Although our results suggest that changes in atmospheric circulation play an important role, we do not exclude that other processes, like an increase in aerosol lifetime in the atmosphere due to change of the hydrological cycle during negative IPO phase, could be responsible for part of the IPO signal in Greenland ice cores.

The air temperature and atmospheric circulation patterns associated with ice core Ca^{2+} records from northern Greenland during the last 400 years resemble the corresponding observational patterns. Also, in this case, the most stable pattern is recorded in the Pacific realm. Negative (positive) IPO phase is associated with higher (lower) probability of relatively high (low) dust, concentration in northern Greenland. This result is supported also by the negative correlation between our dust record and a recent ice-core based IPO reconstruction (Figure S6 in Supporting Information S1). The agreement with the IPO reconstruction of Porter et al. (2021) alleviates concerns regarding possible time scale errors in our ice core dust records. Furthermore, the results remain unchanged if revised scale ages of B16, B18, and B21 records, as presented in recent studies (Weisbach et al., 2016) are considered in the analysis (not shown).

In this study, we report a robust IPO signal in low resolution ice core dust concentration records from northern Greenland during the last 400 years. This conclusion is based on a limited number of ice core records from northern Greenland. It needs further observational and modeling studies to disentangle the physical mechanisms behind this statistical link. Understanding the changes in dust uptake, transport and deposition patterns in northern Greenland is significant for the interpretation of ice core dust records in terms of climate variability as well as for the reconstruction of the IPO index using long ice core records from this region.

Data Availability Statement

The data that support the findings of this study are openly available. The relevant papers associated with these datasets are indicated in the text. The data links are as follows:

1. Ice cores:

   B16 https://doi.org/10.1594/PANGAEA.57092.
   B21 https://doi.org/10.1594/PANGAEA.57294.
   B18 https://doi.org/10.1594/PANGAEA.107285.
   GISP2 https://doi.org/10.1594/PANGAEA.55536.
   NEEM-2011-S1 https://arcticdata.io/catalog/view/doi%3A10.18739%2FA2ST7DX9N.

2. Dust mass concentration (Dusmass) and 500 hPa geopotential height (Z500) https://disc.gsfc.nasa.gov/datasets?project=MERRA-2.
3. Sea Surface Temperature (SST) https://psl.noaa.gov/data/gridded/data.cobe.html.
4. 20CRv2c reanalysis (Z500 and wind) https://psl.noaa.gov/data/gridded/data.20thC_ReanV2c.html.
5. IPO reconstruction (Porter et al., 2021) https://www.ncdc.noaa.gov/paleo-search/study/33092.
6. EKF400v2 (Valler et al., 2021) https://www.wdc-climate.de/ui/entry?acronym=EKF400_v2.0.

Acknowledgments
NR, MI, and GL are supported by Helmholtz funding through the joint program "Changing Earth—Sustaining our Future" (PoF IV) program of the AWI. Funding by Helmholtz Climate Initiative—REKLIM is gratefully acknowledged. We acknowledge support by the Open Access Publication Funds of Alfred-Wegener-Institut Helmholtz-Zentrum für Polar- und Meeresforschung. We thank all researchers who made the data sets used in this study available. We would like also to thank the reviewers for their thoughtful comments that lead to a significant improvement of our manuscript. Open Access funding enabled and organized by Projekt DEAL.

References

Bory, A., Biscaye, P., Svensson, A., & Grousset, F. (2002). Seasonal variability in the origin of recent atmospheric mineral dust at NorthGRIP, Greenland. *Earth and Planetary Science Letters*, *196*(3–4), 123–134. https://doi.org/10.1016/S0012-821X(01)00609-4

Bullard, J. E., & Mockford, T. (2018). Seasonal and decadal variability of dust observations in the Kamgerlussuaq area, west Greenland. *Arctic Antarctic and Alpine Research*, *50*(1), e1415854. https://doi.org/10.1080/15230430.2017.1415854

Chiapello, I., Moulin, C., & Prospero, J. M. (2005). Understanding long-term variability of African dust transport across the Atlantic as recorded in both Barbados surface concentrations and large-scale total ozone mapping spectrometer (TOMS) optical thickness. *Journal of Geophysical Research*, *110*(D18), D18S10. https://doi.org/10.1029/2004JD005132

Clifford, H. M., Spaulding, N. E., Kurbatov, A. V., More, A., Korotkikh, E. V., Sneed, S. B., et al. (2019). A 2000 year Saharan dust event proxy record fropm an ice core in the European Alps. *Journal of Geophysical Research: Atmosphere*, *124*(23), 12882–12900. https://doi.org/10.1029/2019JD030725

Compo, G. P., Whitaker, J. S., Sardeshmukh, P. D., Matsui, N., Allan, J., Yin, X., et al. (2011). The twentieth century reanalysis project. *Quarterly Journal of the Royal Meteorological Society*, *137*(654), 1–28. https://doi.org/10.1002/qj.776

Fischer, H. (2000a). Chemistry of ice core ngt03C93.2 from the North Greenland Traverse. *PANGAEA*. https://doi.org/10.1594/PANGAEA.57092

Fischer, H. (2000b). Chemistry of ice core ngt27C94.2 from the North Greenland Traverse. *PANGAEA*. https://doi.org/10.1594/PANGAEA.57294

Fischer, H. (2003). Chemistry of ice core ngt14C93.2 from the North Greenland Traverse. *PANGAEA*. https://doi.org/10.1594/PANGAEA.107285

Fischer, H., Siggaard-Andersen, M. L., Ruth, U., Röthlisberger, R., & Wolf, E. (2007). Glacial/interglacial changers in mineral dust and sea-salt records in polar ice cores: Sources, transport and deposition. *Reviews of Geophysics*, *45*(1), RG1002. https://doi.org/10.1029/2005RG000192

Francis, D., Eayrs, C., Chaboureau, J. P., Mote, T., & Holland, D. (2019). A meandering polar jet caused the development of a Saharan cyclone and the transport of dust toward Greenland. *Advance Scientific Research*, *16*, 49–56. https://doi.org/10.5194/asr-16-49-2019

Fuhrer, K., Wolf, E. W., & Johnsen, S. J. (1999). Timescales for dust-variability in the Greenland Ice Core Project (GRIP) ice core in the last 100, 000 years. *Journal of Geophysical Research: Atmosphere*, *104*(D24), 31043–31052. https://doi.org/10.1029/1999JD900929

Gelaro, R., McCarty, W., Suárez, M. J., Todling, R., Molod, A., Takacs, L., et al. (2017). The Modern Eran Retrospective Analysis for Research and Applications, version 2 (MERRA-2). *Journal of. Climate*, *30*(14), 5419–5454. https://doi.org/10.1175/JCLI-D-16-0758.1

Gong, D. Y., Mao, R., & Fan, Y. D. (2006). East Asian dust storm and weather disturbance: Possible links to the Arctic Oscillation. *International Journal of Climatology*, *26*(10), 1379–1396. https://doi.org/10.1002/joc.1324

Hamilton, W. L., & Langway, C. C. Jr. (1967). A correlation of microparticle concentrations with oxygen isotope ratios in 700 year old Greenland ice. *Earth and Planetary Science Letters*, *3*, 363–366. https://doi.org/10.1016/0012-821X(67)90062-3

Hand, J. L., White, W. H., Gebhart, K. A., Hyslop, N. P., Gill, T. E., & Schitchel, B. A. (2016). Early onset of the fine spring dust season in the southwestern United States. *Geophysical Research Letters*, *43*(8), 4001–4009. https://doi.org/10.1002/2016GL068519

Henley, A., Gergis, J., Karoly, D. J., Power, S., Kennedy, J., & Folland, C. K. (2015). A tripole index for interpacific decadal oscillation. *Climate Dynamics*, *45*(11–12), 3077–3090. https://doi.org/10.1007/s00382-015-2525-1

Huang, Z., Huang, J., Hayasaka, T., Wang, S., Zhou, T., & Jin, H. (2015). Short-cut transport path for Asian dust directly to the Arctic: A case study. *Environmental Research Letters*, *10*(11), 114018. https://doi.org/10.1088/1748-9326/10/11/114018

Intergovernmental Panel on Climate Change (IPCC). (2007). Intergovernmental panel on climate change (IPCC). In S. Solomon, D. Quin, M. Mannung, M. Marquis, K. Averyt, et al. (Eds.), *Climate change: The physical science basis*. Cambridge University Press UK.

Ishii, M., Shouji, A., Sugimoto, S., & Matsumoto, T. (2005). Objective analyses of sea-surface temperature and marine meteorological variables for the 20th century using ICOADS and the kobe collection. *International Journal of Climatology*, *25*(7), 865–879. https://doi.org/10.1002/joc.1169

Kjaer, H. A., Zens, P., Black, S., Lund, K. H., Svensson, A., & Vallelonga, P. (2022). Canadian forest fires, Icelandic volcanoes and increased local dust observed in six shallow Greenland firn cores. *Climate of the Past*, *18*(10), 2211–2230. https://doi.org/10.5194/cp-18-2211-2022

Kok, J. F., Adebiyi, A. A., Albani, S., Balkanski, Y., Checa-Garcia, R., Chin, M., et al. (2021). Contribution to the world's main dust source regions to the global cycle of desert dust. *Atmospheric Chemistry and Physics*, *21*(10), 8169–8193. https://doi.org/10.5194/acp-21-8169-2021

Legrand, M., & Mayewski, P. (1997). Glaciochemistry of polar ice cores: A review. *Review of Geophysics*, *35*(3), 219–243. https://doi.org/10.1029/96RG03527

Mayewski, P. A. (1999). GISP2 ions: B core (0-200 meters). *PANGAEA*. https://doi.org/10.1594/PANGAEA.55536

McConell, J. R. (2013). Elemental and chemical measurements of the Northern Greenland Eemian Ice Drilling core, NEEM-2011-S1, collected in summer 2011 near the NEEM deep drilling site in northwest Greenland. *Arctic Data Center*. https://doi.org/10.18739/A2ST7DX9N

Nagatsuka, N., Goto-Azuma, K., Tsushima, A., Fujita, K., Matoba, S., Onuma, Y., et al. (2021). Variations in mineralogy of dust in an ice core obtained from northwestern Greenland over the past 100 years. *Climate of the Past*, *17*(3), 1341–1362. https://doi.org/10.5194/cp-17-1341-2021

Notaro, M., Yu, Y., & Kalashinikova, O. V. (2015). Regime shift in Arabian dust activity, trigerred by persistent Fertile Crescent drought. *Journal of Geophysical Research*, *120*, 10229–10249. https://doi.org/10.1002/2015JD023855

Porter, S., Mosley-Thompson, E., Thompsopn, L. G., & Wilson, B. (2021). Reconstructing an Interdecadal Pacific Oscillation Index from a Pacific basin-wide collection of ice core records. *Journal of Climate*, *34*(10), 3839–3852. https://doi.org/10.1175/JCLI-D-20-0455

Prospero, J. M., Ginoux, P., Torres, O., Nicholson, S. E., & Gill, T. E. (2002). Environmental characterization of global sources of atmospheric soil dust identified with Nimbus 7 total ozone mapping spectrometer (TOMS) absorbing aerosol product. *Reviews of Geophysics*, *40*(1), 2-1–2-31. https://doi.org/10.1029/2000RG000095

Pu, B., & Ginoux, P. (2016). The impact of the Pacific Decadal Oscillation on springtime dust activity in Syria. *Atmospheric Chemistry and Physics*, *16*(21), 13431–13448. https://doi.org/10.5194/acp-16-13431-2016

Rasmussen, S. O., Bigler, M., Blockley, S. P., Blunier, T., Buchardt, S. L., Clausen, H. B., et al. (2014). A stratigraphic framework for abrupt climatic changes during the last glacial period based on three synchronized Greenland ice-core records: Refining and extending the INTIMATE event stratigraphy. *Quaternary Science Reviews*, *106*, 14–28. https://doi.org/10.1016/j.quascirev.2014.09.007

Rodriguez, S., Cuevas, E., Prospero, J. M., Alastuey, A., Querol, X., Lopez-Solano, J., et al. (2015). Modulation of Saharan dust export by the North African dipole. *Atmospheric Chemistry and Physics*, *15*(13), 7471–7486. https://doi.org/10.5194/acp-15-7471-2015

Shi, L., Zhang, J., Zhang, D., Wang, J., Meng, X., Liu, Y., & Yao, F. (2022). What cause the interdecadal shift in the El Nino-Southern Oscillation (ENSO) impact on dust mass concentration over northwestern South Asia? *Atmospheric Chemistry and Physics*, *22*(17), 11255–11274. https://doi.org/10.5194/acp-22-11255-2022

Steffensen, J. P. (1997). The size distribution of microparticles from selected segments of Greenland Ice Core Project ice core representing different climatic periods. *Journal of Geophysical Research*, *102*(C12), 26755–26763. https://doi.org/10.1029/97JC01490

Valler, V., Franke, J., Brugnara, Y., & Broenimann, S. (2021). An updated global atmospheric paleo-reanalysis covering the last 400 years. *Geoscience Data Journal*, *9*(1), 89–107. https://doi.org/10.1002/gdj3.121

von Storch, H., & Zwiers, F. W. (1999). *Statistical analysis in climate Research*. Cambridge University Press. https://doi.org/10.1017/CBO9780511612336

Wallace, J. M., & Gutzler, D. S. (1981). Teleconnections in the geopotential height field during the northern Hemisphere winter. *Monthly Weather Review*, *109*(4), 784–812. https://doi.org/10.1175/1520-0493(1981)109<0784:TITGHF>2.0.CO;2

Weißbach, S., Wegner, A., Opel, T., Oerter, H., Vinther, B. M., & Kipfstuhl, S. (2016). Spatial and temporal oxygen isotope variability in northern Greenland—Implications for a new climate record over the past millennium. *Climate of the Past*, *12*(2), 171–188. https://doi.org/10.5194/cp-12-171-2016

Yu, S., & Sun, J. (2020). Potential factors modulating ENSO's influences on the East Asian trough in boreal winter. *International Journal of Climatology*, *40*(12), 5066–5083. https://doi.org/10.1002/joc.6505

Yu, Y., Notaro, M., Liu, Z., Wang, F., Alkolibi, F., Fadda, E., & Bakhrjy, F. (2015). Climatic controls on the interannual to decadal variability in Saudi Arabian dust activity: Toward the development of a seasonal dust prediction model. *Journal of Geophysical Research: Atmosphere*, *120*(5), 1739–1758. https://doi.org/10.1002/2014/D022611